

DESIGNS FOR A LINAC-RING LHeC

F. Zimmermann, O. Brüning, E. Ciapala, F. Haug, J. Osborne, D. Schulte, R. Tomas, CERN, Switzerland; C. Adolphsen, Y.-P. Sun, SLAC, USA; R. Calaga, V. Litvinenko, BNL, USA; J. Dainton, M. Klein, Liverpool U., UK; S. Chattopadhyay, Cockcroft Institute, UK; A. Eide, NTNU, Norway

Abstract

We consider three scenarios for the recirculating electron linear accelerator (RLA) of a linac-ring type electron-proton collider based on the LHC (LHeC): i) a pulsed linac with a final beam energy of 60 GeV [“p-60”], ii) a higher luminosity configuration with two cw linacs and energy-recovery (ERL) also at 60 GeV [“erl”], and iii) a high energy option using a pulsed linac with 140-GeV final energy [“p-140”]. We discuss parameters, synchrotron radiation, footprints, and performance for the three scenarios.

INTRODUCTION

Since 2007, the design study for a Large Hadron electron Collider (LHeC) [1, 2, 3, 4, 5] proceeds under an ECFA mandate. The LHeC collider would bring into collision the 7-TeV protons of the Large Hadron Collider (LHC), presently being commissioned at CERN, with an electron or positron beam of energy 60–140 GeV. The minimum target luminosity ranges from $10^{32} \text{ cm}^{-2}\text{s}^{-1}$ to $10^{33} \text{ cm}^{-2}\text{s}^{-1}$, varying with the angular acceptance of the detector for different physics goals. Lepton beam polarization is also desired.

Two options for realizing such collider are: (1) a “Ring-Ring” (RR) option with a new lepton ring in the LHC tunnel [6, 7]; and (2) a “Linac-Ring” (LR) option based on a superconducting electron linac, configured as a recirculator [5, 8]. This paper focuses on the LR LHeC.

The electron beam size is matched to the size of the protons, $\sigma_p^* = \sigma_e^*$. For round beams the luminosity is

$$L = \frac{1}{4\pi e} \frac{N_{b,p}}{\epsilon_p} \frac{1}{\beta_p^*} I_e H_{\text{hg}}, \quad (1)$$

where e denotes the electron charge, and the subindices p or e refer to protons or electrons (positrons). The luminosity (1) depends only on the p-beam brightness ($N_{b,p}/\epsilon_p$) with $N_{b,p}$ the number of protons per bunch and ϵ_p the geometric emittance, on β_p^* , on the electron beam current I_e , and on the hourglass factor H_{hg} . The term ($N_{b,p}/\epsilon_p$) is limited by space charge in the proton injector complex and by the pp beam-beam tune shift. The electron current I_e is limited by the available electrical power. The proton IP beta function β_p^* is confined, on the proton side, by the IR layout, and on the electron side by the reduction factor due to the hourglass effect, H_{hg} . For zero crossing angle and $\sigma_{z,p} \gg \sigma_{z,e}$, $H_{\text{hg}}(z) = \sqrt{\pi} z e^{z^2} \text{erfc}(z)$ with $z \equiv 2(\beta_e^*/\sigma_{z,p})(\epsilon_e/\epsilon_p)/\sqrt{1 + (\epsilon_e/\epsilon_p)^2}$. There is no lower bound on ϵ_e , as the linac beam collides only once, and, even with pessimistic assumptions on the linac emit-

tance, the hourglass reduction remains acceptable for β_p^* values as low as 0.1 m [8].

The nominal LHC beam consists of trains of bunches with 1.15×10^{11} protons each, spaced at 25 ns. An alternative LHC beam, delivering the same nominal pp luminosity, would use bunches with the “ultimate” population of 1.7×10^{11} protons spaced at 50 ns [9]. One of the “Super-LHC” upgrade scenarios, called the Large Piwinski Angle (LPA) scheme, is also based on 50-ns spacing, but with 4.2×10^{11} protons per bunch. The LHeC luminosity is directly proportional to the proton bunch intensity, which is 1.5 or 3.7 times higher than the nominal LHC value for the alternative proton beam and the LPA beam, respectively. The proton IP beta function for the LR LHeC is taken to be $\beta_{x,y}^* = 0.1 \text{ m}$ [10, 11, 12].

For the purpose of performance estimates, the electrical wall-plug power available for the lepton beam is held constant, equal to 100 MW, for all scenarios. To first order, the luminosity scales linearly with this power.

Table 1: LHC Proton Beam Scenarios. “LHC” refers to the nominal LHC, “LHC*” to the alternative scenario and “LPA” to the SLHC scenario with large Piwinski angle [9].

	$N_{b,p}$	T_{sep}	$\epsilon_p \gamma_p$
LHC	1.1×10^{11}	25 ns	$3.75 \mu\text{m}$
LHC*	1.7×10^{11}	50 ns	$3.75 \mu\text{m}$
LPA	4.2×10^{11}	50 ns	$3.75 \mu\text{m}$

LINAC & ARC PARAMETERS

The most important features of each LR design are the size of the linac complex (which depends on the accelerating gradient, the beam energy, and on the potential inclusion of energy recovery) and the electrical wall-plug power required for a given luminosity. Electrical power is needed for the linac cryogenics (again depending on the gradient), and for the RF systems. The latter must sustain a certain beam power, control microphonics, and compensate for energy loss from synchrotron radiation (SR) in the return arcs.

From the three scenarios considered, two (p-60 and p-140) are pulsed linacs with an ILC-like cavity gradient of 31.5 MV/m; the third one (erl) operates in CW mode with a cavity gradient of 18 MV/m. For the linac we assume a packing factor F of 0.57, which translates the cavity gradient into a real-estate gradient. We assume a SC linac RF frequency of 700 MHz, similar to eRHIC, SPL, and ESS. The linac parameters, summarized in Table 2, are taken, or scaled, from the eRHIC (5-cell) [13] and ILC (9-cell) cavity designs. The pulsed linacs in the p-60 and p-140 sce-

narios could alternatively operate at the ILC RF frequency of 1.3 GHz. A pulsed-linac gradient of 31.5 MV/m corresponds to the ILC design target value. For the erl scenario the RF power quoted is used for controlling microphonics. Another 50 MW electrical wall-plug power would be available to compensate for energy recovery inefficiencies of up to about 6% (half of which is already expected from synchrotron radiation; see Table 3). With a total cryo power ranging from 10 to 25 MW for the three scenarios (Table 2), we anticipate that between two and six 4–5 MW cryo-plants will be required.

Table 2: SC Linac Parameters. †: w/o 4 & 40-K cooling; *RT: room temperature; ‡: w/o recovery inefficiency

	p-60	erl	p-140
RF frequency [MHz]	700	700	700
cavity length [m]	1	1	1
energy gain / cavity [MeV]	31.5	18	31.5
R/Q [100 Ω]	≥ 4	≥ 4	≥ 4
Q_0 [10^{10}]	1	2.5	1
power loss, stat [W/cav.]	5	5	5
power loss, RF [W/cav]	12.3	32	12.3
power loss, total [W/cav]	17.3	37.2	17.3
real-est. gradient [MeV/m]	17.8	10.26	17.8
length/GeV [m]	55.7	97.5	55.7
#cavities/(1 GeV)	31.8	55.6	31.8
power loss/GeV (2 K) [kW]	0.55	2.06	0.55
“W per W” (1.8 K to RT*)	600	600	600
power loss/GeV (RT*) [MW]	0.33	1.24	0.3
final energy [GeV]	60	60	140
# passes for acceleration	2	3	2
# passes for deceleration	0	3	0
total linac length [km]	1.67	1.95	3.90
tot. cryo power [‡] (RT*) [MW]	9.9	24.75	23.1
av. beam current [mA]	0.74	6.6	0.27
beam power at IP [MW]	45	396	39
RF power [MW]	89	22 [†]	75.6
cryo + RF power [MW]	99	47 [†]	98.4

Table 3 presents the SR energy loss for the 3 layouts assuming different bending radii as well as the additional RF power needed to compensate for these losses. In the ERL case, this compensation can be done via a higher-harmonic 1.4-GHz RF system (as for eRHIC [13]). The total wall-plug power is the sum of the cryo power, the accelerating RF power (i.e. the part of the accelerating RF power that is not recovered), and the SR-compensating RF power.

The beam energy of the erl scenario can be increased to 70 GeV, by lengthening the two linacs from 1950 to 2275 m, at constant accelerating gradient, and by increasing the cryo and RF power in Table 2 to 29 MW and 25.9 MW, respectively. The SR-compensating RF power would almost double, to 50.3 MW, for equal current and bending radius.

FOOTPRINTS

For the erl scenario it is advantageous to split the linac into two, placed on either straight of a racetrack. The ad-

Table 3: Arc Parameters

	p-60	erl	p-140
bending radius [km]	0.12	0.7	0.7
rel. SR loss [%]	1.0	1.0 (IP)	2.2
total SR loss [GeV]	0.6	2.06	3.0
		(0.6 to IP)	
dipole packing	0.7	0.7	0.7
effective radius [km]	0.17	1.0	1.0
comp. RF freq. [GHz]	0.7	1.4	0.7
add'l RF power [MW]	0.9	27.2	1.65

vantages are a reduction in the total length of the accelerator footprint and reduced losses due to synchrotron radiation in the highest-energy arc, which only bends by 180° instead of 360°. To further reduce the dimensions the beam is accelerated during 3 passages through the linac. In the case of the pulsed linac scenarios (p-60, p-140) an optimization for cost and synchrotron radiation [14] shows that, for the lepton energy range considered, passing two times through a single linac is the most efficient solution, which, for the linacs without energy recovery, also minimizes the maximum beam energy in the return arcs. These configurations have been assumed for Table 3. Footprints of the three scenarios are sketched in Fig.1. For the p-60 scenario, alternative footprints would be a dogbone or (with a view to polarization [15]) a figure-of-eight, where the return straight and linac would share a tunnel.

LINAC BEAM

Draft linac optics for various versions of recirculating linacs with and without energy recovery have been developed for a linac injection energy of 0.5 GeV [16, 17]. Further optimization, in particular of the optics in the transition regions, is possible.

The e^- beam for the linac can be produced from a polarized dc gun with an initial normalized rms emittance between 10 and 50 μm . Without polarization even smaller emittances can be obtained from a photo RF gun. Positron sources are under consideration.

Tracking simulations of the multiple linac passes using the draft optics were performed with a modified version of MAD-X assuming an initial incoherent rms energy spread of 10^{-4} , 300 μm rms bunch length, and an initial normalized emittance ranging from 2 μm or 200 μm [18, 19]. The simulation results demonstrate that the emittance growth due to energy spread and chromaticity is negligible. For the 60-GeV designs, the emittance growth from synchrotron radiation also remains small, at the level of 1-2% for an emittance of 50 μm . For the 140 GeV optics, synchrotron radiation leads to an emittance increase by about 50 μm , almost independent of the initial emittance value. Assuming an initial value of 50 μm the emittance then doubles at the IP.

The electron-beam emittance after the ep collision remains small enough for deceleration down to the injection energy [8], which is important for energy recovery.

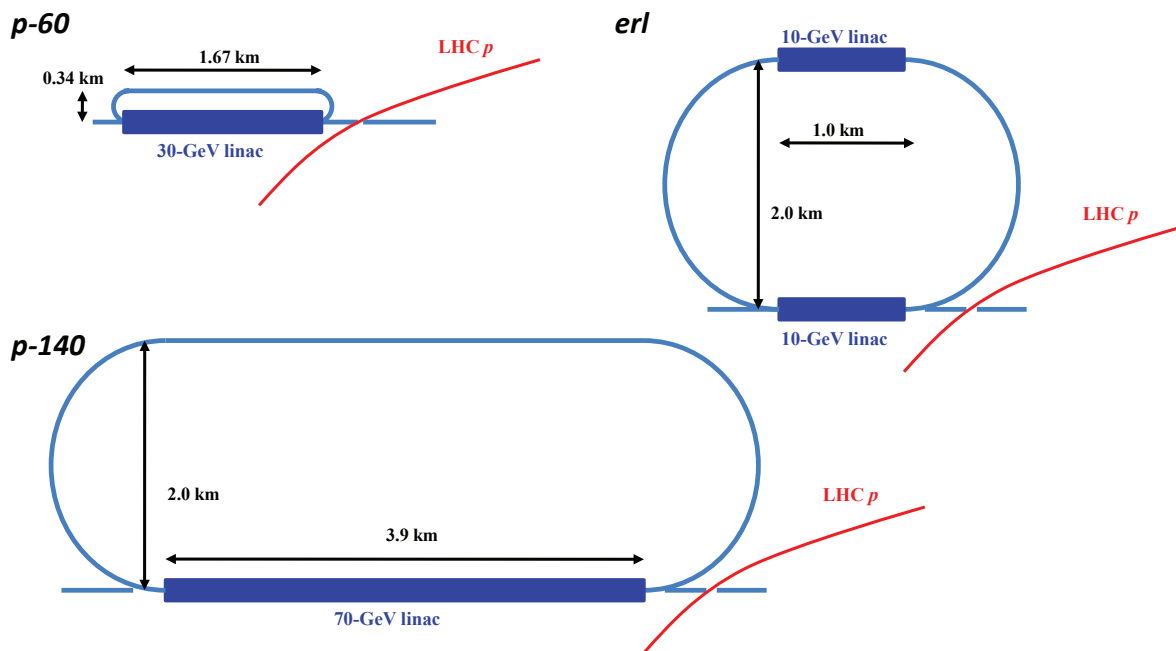


Figure 1: Footprints for three LHeC scenarios based on recirculating SC linac(s).

PERFORMANCE & BASELINE

Table 4 summarizes the lepton-beam parameters and luminosity performance; see also [2, 4, 8, 5]. The luminosity numbers assume the ultimate LHC bunch intensity of 1.7×10^{11} as for LHC* in Table 1, but they are independent of the proton bunch spacing (25 or 50 ns). They would be 33% lower for the nominal LHC beam, and 2.5 times higher for the LPA beam. The LHeC luminosity could be significantly increased by reducing the LHC proton beam emittance, e.g. through advanced cooling techniques [13], if or when the latter become operational. The 60-GeV “erl” scenario, with a possible extension to 70 GeV, has been chosen as baseline for the linac-ring LHeC design.

Table 4: Lepton Beam Parameters and Luminosity

	p-60	erl	p-140
e^- energy at IP [GeV]	60	60	140
luminosity [$10^{32} \text{ cm}^{-2} \text{ s}^{-1}$]	1.1	10.1	0.4
polarization [%]	90	90	90
bunch population [10^9]	4.5	2.0	1.6
e^- bunch length [μm]	300	300	300
bunch interval [ns]	50	50	50
transv. emit. $\gamma\epsilon_{x,y}$ [μm]	50	50	100
rms IP beam size [μm]	7	7	7
hourglass reduction H_{hg}	0.91	0.91	0.94
crossing angle θ_c	0	0	0
repetition rate [Hz]	10	CW	10
bunches/pulse [10^5]	1	N/A	1
pulse current [mA]	16	10	6.6
beam pulse length [ms]	5	N/A	5
ER efficiency η	0	94%	0
total wall plug power [MW]	100	100	100

REFERENCES

- [1] LHeC web site: <http://cern.ch/lhec>
- [2] First ECFA-CERN LHeC Workshop, Divonne, Sept. 2008.
- [3] J. Dainton *et al*, Proc. EPAC'08 Genoa, p. 1903 (2008).
- [4] 2nd ECFA-CERN LHeC Workshop, Divonne, Sept. 2009.
- [5] F. Zimmermann *et al*, FRIPBO5, PAC'09 Vancouver,
- [6] J.B. Dainton *et al*, JINST 1: P10001 (2006).
- [7] F. Willeke *et al*, Proc. EPAC'08 Genoa, p. 2638 (2008).
- [8] F. Zimmermann *et al*, *ibid.*, p. 2847 (2008).
- [9] F. Zimmermann, “Parameter Space Beyond 10^{34} ,” Proc. LHC Performance Workshop Chamonix 2010.
- [10] R. Tomas, “IR Design for LR,” in [4].
- [11] M. Korostelev, private communication (2010).
- [12] F. Zimmermann *et al*, “Interaction-Region Design Options for a Linac-Ring LHeC,” these proceedings.
- [13] V. Litvinenko, “Future Electron-Proton(Ion) Colliders,” this conference.
- [14] J. Skrabacz, CERN-AB-Note-2008-043 (2008).
- [15] Ya. Derbenev, Proc. EPAC'02 Paris, p. 314 (2002).
- [16] A. Eiders, “Optics Development for the Recirculating Linac of a High-Energy Hadron-Lepton Collider (LHeC) at the LHC,” NTNU Project Thesis (2009)
- [17] Y. Sun *et al*, “Lattice Design for the LHeC Recirculating Linac,” this conference.
- [18] Y. Sun, “Emittance Growth in the LHeC Recirculating Linac,” this conference.
- [19] Y. Sun, “Emittance Growth in the LHeC Recirculating Linac,” in [4].